Proteomic Analysis of Aqueous Humor Reveals Changes in Extracellular Matrix Pathways in Proliferative Diabetic Retinopathy Patients Treated with Intravitreal Ranibizumab

Xiaolan Du[1,2], Huan Chen[1,2], Tan Wang[1,2], and Hanyi Min[1,2,*]

1 Department of Ophthalmology, Peking Union Medical College Hospital, Chinese Academy of Medical Sciences and Peking Union Medical College, Beijing 100730, China;

2 Key Laboratory of Ocular Fundus Diseases, Chinese Academy of Medical Sciences and Peking Union Medical College, Beijing 100730, China;

* Correspondence: minhy@pumch.cn; Tel.: +86-18601367871; Fax: +86-01069156815.

Abstract

Anti-VEGF therapy is commonly used to treat proliferative diabetic retinopathy (PDR), but the exact mechanism of VEGF signaling is not fully understood. Using data-independent acquisition mass spectrometry (DIA-MS), we analyzed proteomic changes in aqueous humor (AH) samples collected before and one week after intravitreal ranibizumab (IVR) treatment from 10 PDR patients to discover potential biomarkers. Resultantly, 875 proteins were quantified and 26 proteins were significantly altered in response to IVR treatment in PDR. Further investigation through gene ontology (GO) and pathway analysis revealed that these differentially expressed proteins were primarily involved in extracellular matrix (ECM) and platelet degranulation signaling. Protein-protein interaction analysis highlighted five hub proteins (COL3A1, DPT, VEGFA, SPP1, SERPING1) that were found to be ECM components. Enzyme-linked immunosorbent assay (ELISA) confirmed the decreased levels of VEGFA and increased levels of DPT proteins after IVR treatment in another 8 samples of AH in 4 PDR patients. Our study provided novel insights into aqueous proteins of PDR following IVR treatment. Targeting the ECM pathway, particularly the elevation of DPT protein, may provide a deeper understanding of the anti-VEGF resistance and VEGF signaling in PDR.

Keywords: Proliferative diabetic retinopathy; Extracellular matrix; Ranibizumab; Data-independent acquisition; Aqueous humor

1. Introduction

Proliferative diabetic retinopathy (PDR) is a leading cause of vision loss and blindness in the working population, characterized by abnormal neovascularization and subsequent fibrosis, leading to vitreous hemorrhages (VH) and tractional retinal detachment (TRD) (Antonetti et al., 2021; Sharma et al., 2022; Soni et al., 2021). Inhibition of retinal neovascularization is the core of DR prevention and treatment, and abnormal vascular endothelial growth factor (VEGF) production is a hallmark of angiogenesis (Li et al., 2019). Therefore, intraocular VEGF inhibitor therapies have become the first choice for DR complications (Matonti et al., 2022; Mukwaya et al., 2021). In patients with PDR indicated for vitrectomy, a 3 to 7-day preoperative anti-VEGF agent (e.g. Ranibizumab, Conbercept, and Aflibercept) is commonly applied to reduce intraoperative and postoperative bleeding and increase the success rate of the operation (Li, Guo, et al., 2022; Li, Tang, et al., 2022; Smith & Steel, 2015; Wang et al., 2020).

Although there has been widespread use of anti-VEGF treatment, increasing clinical investigations have indicated that the efficacy of intravitreal anti-VEGF treatment varies greatly, as no efficacy was observed and even exacerbated fibrosis and TRD after intraocular injection in some patients with PDR (Chatziralli & Loewenstein, 2021; Dong et al., 2021; Mukwaya et al., 2021; Tan et al., 2021; Tsui et al., 2023). This suggests that anti-VEGF mono-therapy is not sufficient to regress angiogenesis and fibrosis. Interestingly, few laboratory experiments have indicated that combining anti-VEGF therapy with other factors, such as apolipoprotein A-I/apoA-I binding protein, pigment epithelium-derived factor, and müller glia-derived exosomal miR-9-3p, may be more effective than monotherapy in inhibiting vascular regrowth and overcoming anti-VEGF resistance (Liu et al., 2022; Xi, 2022; Zhang et al., 2022). Recent research has indicated that anti-VEGF treatment in PDR can alter the levels of certain intravitreal and aqueous proteins, including secreted phosphoprotein 1 (SPP1), placenta growth factor (PIGF), apolipoprotein C-I (APOC1), serpin peptidase inhibitor clade A member 5 (SERPINA5), keratin 1 (KRT1), and apolipoprotein A-II (APOA2) (Hu et al., 2022; Loukovaara et al., 2015; B. N. Zhang et al., 2021; Zhang et al., 2020; Zou, Han, et al., 2018; Zou, Zhao, et al., 2018). Our previous studies have also found that aldehyde dehydrogenase family 3 member A1 (ALDH3a1), haptoglobin (HP) were increased after anti-VEGF treatment in aqueous humor of PDR(Chen, Qiu, et al., 2022; Wang et al., 2023). However, the exact role of these candidate molecules and the underlying

mechanism of anti-VEGF resistance still require further investigation and a comprehensive understanding.

Ranibizumab is a monoclonal antibody that specifically binds to all isoforms of VEGF-A(Li, Guo, et al., 2022; Li, Tang, et al., 2022). Han and colleagues discovered that intravitreal ranibizumab (IVR) treatment leads to changes in the levels of vitreous proteins in PDR, including increased levels of APOC1, SERPINA5, and KRT1, and decreased levels of TIMP2 and VEGFA, while “innate immune response” and “platelet degranulation” were the notable pathways in response to IVR (Zou, Han, et al., 2018). Furthermore, proteomic research by She et al. suggested that IVR treatment could potentially stimulate SPP1 expression via the "GnRH secretion" and "Circadian rhythm" signaling pathways against PDR development (She et al., 2022). However, it is still unclear whether ranibizumab also causes changes in the protein profile of the aqueous humor in patients with PDR, further exploration is needed to understand the mechanisms of intravitreal ranibizumab (IVR).

To gain deeper insights into the molecular mechanisms underlying anti-VEGF therapy and to identify potential aqueous proteins associated with IVR treatment, our study employed data-independent acquisition (DIA) methods to analyze proteomic changes in the aqueous humor of ten PDR patients before (Pre group) and after (Post group) IVR treatment, and further verification of candidate proteins were conducted using ELISA on four additional independent PDR patients (Figure 1).

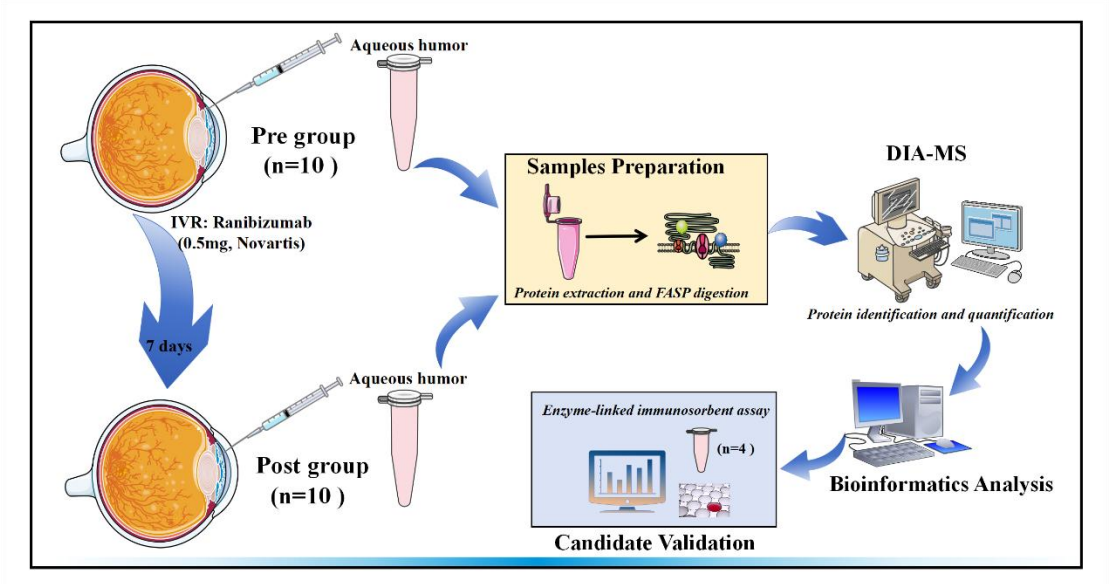

Figure 1 Study design and proteomics pipeline for aqueous humor before and after IVR treatment in PDR.

A total of 28 aqueous humor samples were collected from 14 PDR patients, both before (Pre group) and after (Post group) IVR treatment, by the Hanyi Min team at Peking Union Medical College Hospital (PUMCH). Twenty paired samples from 10 PDR patients were sent to BIOMS (Beijing, China) for data-independent acquisition mass spectrometry (DIA-MS) analysis. Bioinformatics analysis was then performed to investigate the functional tendencies of differentially expressed proteins (DEPs) and abnormal molecular networks. Finally, enzyme-linked immunosorbent assay (ELISA) was used to validate the changes in hub proteins in the aqueous humor of an additional 4 PDR patients.

2. Experimental Procedures

2.1 Participants

The study was a prospective, paired before/after study. From March 2019 to October 2021, a total of 14 patients with PDR who were indicated for vitrectomy were recruited from the Peking Union Medical College Hospital (PUMCH) and informed consent was obtained from each subject after a complete explanation of the nature and possible consequences of the study, of which 10 patients for DIA-MS and 4 patients for ELISA analysis. AH was obtained from each patient twice: the first time before IVR treatment was defined as the Pre group, and the second time after one week of IVR treatment was defined as the Post group. Our research was approved by the Ethics Committee of PUMCH (NO. I-22PJ271) following the provisions of the Declaration of Helsinki.

The PDR patients indicated for primary pars plana vitrectomy (PPV) as treatment for vitreous hemorrhages, preretinal membranes, and tractional retinal detachments were enrolled by one retinal specialist (Hanyi Min). We excluded subjects with any other ocular diseases, high myopia, glaucoma, retinal vascular occlusion, ocular trauma, uveitis, or history of any previous ocular surgery such as cataract surgery, or intraocular injection of anti-vascular

endothelial growth factors. All patients were free of other systemic disorders (e.g., hematological system diseases, malignant cancer, and hyperthyroidism) and ongoing infection. All the subjects underwent comprehensive ophthalmologic examinations including best-corrected visual acuity, intraocular pressure, corneal endothelial cell counts, axial length, and B ultrasound.

2.2 Aqueous Humor Sample Collection

Ranibizumab (0.5mg, Novartis) was injected into the vitreous cavity in the 14 eyes with PDR 1 week before vitrectomy. AH samples were acquired from each PDR patient twice as previously described (Chen, Qiu, et al., 2022; Tsao et al., 2021; Wang et al., 2023). After obtaining informed consent, approximately 0.15 mL of aqueous humor samples were obtained before the injection of ranibizumab and at the start of vitrectomy via anterior paracentesis by the same experienced ophthalmologist. All AH samples without any dilution were immediately collected in a 0.5 mL microcentrifuge tube and stored at −80 °C until further proteomic analysis.

2.3 Sample Preparation for LC/MS-MS

AH sample preparation for LC/MS-MS was performed as previously reported (Chen, Qiu, et al., 2022; Liu et al., 2021; Wang et al., 2023). Briefly, the procedure was as follows: (1) protein extraction: after collecting AH samples from ten patients, the AH samples were thawed and centrifuged at 13,000× g at 4 °C for 15 min from −80 °C. The supernatant was transferred to a 3 KD ultrafiltration tube (Millipore, Burlington, MA, USA), and then the lysis buffer (2 M thiourea (Sig-ma-Aldrich, St. Louis, MO, USA), 7 M urea (Amresco 0568-1 Kg, USA), 0.1% 3-[(3-cholamidopropyl) dimethylammonio]-1-propane sulfonate (CHAPS), and protease inhibitor cocktail (Roche Applied Science, Indianapolis, IN, USA)) were used to exchange protein solutions. The protein concentration was determined with a BCA kit (Thermo Fisher 23,236, Waltham, MA, USA) according to the manufacturer's instructions; (2) Filter-aided sample preparation (FASP) digestion: for protein digestion, the protein solution was reduced with 25 mM dithiothreitol (DTT) (Bio-Rad, Hercules, CA, USA) for 60 min at 37 °C and alkylated with 50 mM iodoacetamide for 30 min at room temperature in darkness.

The mixture was transferred into a 10 KDa ultrafiltration filter (Millipore, Burlington, MA, USA). Thereafter, the filter was washed three times using 300 μL of 20 mM triethylammonium bicarbonate buffer (TEAB) (Sigma T7408, Burlington, MA, USA) and centrifuged at 12,000× g for 10 min, and then re-washed using TEAB. Finally, trypsin was added at a trypsin-to-protein mass ratio of 1:50 for digestion overnight and washed three times using TEAB; (3) High pH re-versed-phase (HpRP) chromatography: the digested peptides were resuspended by additional HpRP chromatography. Dried peptides were resuspended in 100 μL of mobile phase A (2% (v/v) acetonitrile (Thermo Fisher, A955-4, Waltham, MA, USA), 98% v/v) ddH2O and pH 10), and then eluted stepwise by injecting mobile B (98% (v/v) acetonitrile, 2% (v/v) ddH2O and pH 10) in the RIGOL L-3000 system (RIGOL, Beijing, China).

2.4 Data-independent acquisition mass spectrometry (DIA-MS)

According to published reports(Chen, Qiu, et al., 2022; Wang et al., 2023; B. N. Zhang et al., 2021), DIA-based proteomic methods were used to identify the protein profiles of the aqueous humor in PDR patients before (pre group, n = 10) and after (post group, n = 10) IVR treatment. The DIA-MS analysis was implemented in BIOMS (Beijing, China).

The DIA analysis principle and theory were described previously(Bons et al., 2023). For MS analysis, samples of 1 μg each were analyzed using an EASY-nLC1000 connected to a Q Exactive HF mass spectrometer (Thermo Fisher, Waltham, MA, USA). Peptides were eluted by using a binary solvent system A (99.9% H2O, 0.1% formic acid (Sigma, Burlington, MA, USA) and B (80% acetonitrile, 19.9% H2O, 0.1% formic acid). The following linear gradient was used:13–28% B for 93 min, 28–38% B for 11 min, 38–100% B for 4 min, and washing with 100% B for 8 min. The eluent was introduced directly to a Q-Exactive HF mass spectrometer via an EASY-Spray ion source. Source ionization parameters were as follows: spray voltage, 2.2 kV; capillary temperature, 320 °C; and declustering potential, 100 V. For DDA MS runs, one full MS scan from 300 to 1600 m/z followed by 20 MS/MS scans were continuously acquired. The resolution for MS was set to 60,000, and that for MS/MS was set to 30,000. The DIA-MS method consisted of an MS1 scan from 300 to 1100 m/z (AGC target

of 3e6 or 80 ms injection time). DIA segments were then acquired at a resolution of 30,000 (AGC target 2e5 and auto injection time). The collision energy was 32%. The spectra were recorded in profile mode.

The identified raw mass spectrometric data from DIA were analyzed with Biognosys' Spectronaut pulsar program(Chen, Qiu, et al., 2022; Chen, Wang, et al., 2022; Wang et al., 2023). The default settings were used for targeted analysis of DIA data in Spectronaut. In brief, the retention time prediction type was set to dynamic iRT (adapted variable iRT extraction width for varying iRT precision during the gradient) and the correction factor for the window. Mass calibration was set to local mass calibration. Decoy generation was set to scramble (no decoy limit). Interference correction on the MS2 level was enabled, removing fragments from quantification based on the presence of interfering signals but keeping at least three fragments for quantification. The false discovery rate (FDR) was estimated with the prophet approach and set to 1 % at the peptide level. Proteome Discoverer 2.3 was used with default settings (Trypsin/P (Promega, V5111, USA), two missed cleavages) to analyze the DDA data. Search criteria included carbamidomethylation of cysteine as a fixed modification and oxidation of methionine and acetyl (protein N terminus) as variable modifications. Initial mass tolerance values for precursor and fragment ions were 10 ppm and 0.02 Da, respectively. The DDA data were searched against the UniProt human database (uniprot_human_73,940_20,190,731_iRT.fasta), and the Biognosys iRT peptides fasta database (uploaded to the public repository). Protein intensity was calculated by summing the intensity of their respective peptides. Proteins identified in more than 50% of the samples in each group were retained for further analysis.

2.3 Bioinformatics Analysis

Protein profiles of the aqueous humor in 10 patients with PDR by DIA analysis were analyzed by Wu Kong online platform (https://www.omicsolution.com/wkomics/main/ accessed on 27 September 2022). Proteins with an adjusted |log2 (fold-change) | >0.58 and *P*-value <0.05 were identified as differentially expressed proteins (DEPs). To explore potential biological functional pathways, the proteomic bioinformatic analysis of GO annotation,

KEGG pathway, REACTOME pathway, and WikiPathways were performed using Metascape web tool (http://metascape.org accessed on 14 January 2023). To further analyze their associations, the DEPs were implemented by Search Tool for the Retrieval of Interacting Genes/Proteins (STRING) (http://string-db.org accessed on 14 January 2023). The results were downloaded and visualized in the form of an interaction network by importing them into Cytoscape Version 3.9.1(Shannon et al., 2003). Hub nodes were selected via four topological analysis methods including degree, edge percolated component (EPC), maximal clique centrality algorithm (MCC), and closeness in Cytoscape plugin cytoHubba(Chin et al., 2014).

2.4 Enzyme-linked immunosorbent assay (ELISA)

To validate the changes of VEGFA and DPT proteins in aqueous humor samples by DIA-MS analysis, the concentrations of proteins were detected by human VEGFA and DPT ELISA kit (Aoxing Bioscience, AX-998787H, AX-530014H, China) following the manufacturer's instructions in AH from the recruited PDR patients. The absorbance was obtained by a microplate reader (BioRad, USA) at 450 nm.

2.5 Statistical analysis

Statistical analysis was conducted by SPSS software version 19.0 (IBM SPSS Statistics 24.0 for Windows, IBM Corp., Armonk, NY, USA) and GraphPad Prism version 9.3.1 for Windows (GraphPad Software, San Diego, California USA, www.graphpad.com accessed on 5 January 2023). Except where indicated otherwise, summary quantitative data were expressed as mean values ± SME and were analyzed by T-text unless otherwise indicated. Differences with a p-value < 0.05 were considered statistically significant.

3. Results

3.1 Clinical characteristics and deferentially abundant proteins

The baseline characteristics of the patients with proliferative diabetic retinopathy (PDR) are presented in Table 1. A total of 14 PDR patients who required vitrectomy were included in our study. Aqueous samples from 10 PDR patients (patients 1-14 in Table 1) were used for DIA-MS analysis, while samples from 4 PDR patients (patients 10-14 in Table 1) were utilized for ELISA analysis. The workflow of proteomic analysis and potential biomarker validation is shown in Figure 1.

In our study, a total of 875 proteins were identified and quantification in AH from the pre and post group by DIA-MS. A comparison of the expression data (Post/Pre group) revealed 26 differentially expressed proteins (DEPs) based on the criteria of |log2 (fold-change)| >0.58 and *p*-value <0.05, including 16 up-regulation proteins and 10 down-regulation proteins in the Volcano plot (Figure 2A). To obtain a better comparison of the global proteomic profiles of aqueous humor in response to IVR, the DEPs were subjected to hierarchical clustering analysis and illustrated the results in an expression heatmap with a dendrogram (Figure 2B). The details of 26 differential proteins, including IDs, gene names, annotations, *P*-value, and fold changes, are shown in Figure 2C.

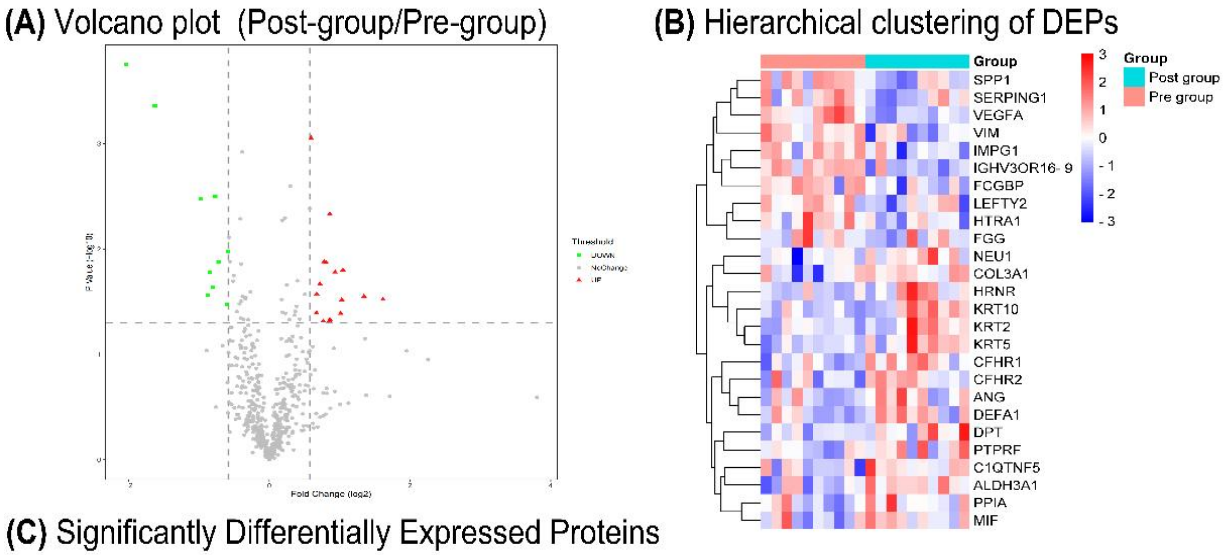

(C) Significantly Differentially Expressed Proteins

Uniport ID	Gene Name	Description	P value	log2(FC)
A0A0B4J2B5	IGHV3OR16-9	Immunoglobulin heavy variable 3/OR16-9 (non-functional) (Fragment)	0.00018	-2.03713
A0A087WUD8	VEGFA	Vascular endothelial growth factor A	0.00043	-1.62616
P10451	SPP1	Osteopontin (Bone sialoprotein 1) (Nephropontin) (Secreted phosphoprotein 1) (SPP-1)	0.00335	-0.97615
B0YJC4	VIM	Vimentin	0.02752	-0.871734
O00292	LEFTY2	Left-right determination factor 2 (Endometrial bleeding-associated factor) (Left-right determination factor A)	0.01664	-0.847215
Q9Y6R7	FCGBP	IgGFc-binding protein (Fcgamma-binding protein antigen) (FcgammaBP)	0.02303	-0.79899
Q17R60	IMPG1	Interphotoreceptor matrix proteoglycan 1 (Interphotoreceptor matrix proteoglycan of 150 kDa)	0.00317	-0.76736
Q92743	HTRA1	Serine protease HTRA1 (EC 3.4.21.-) (High-temperature requirement A serine peptidase 1) (L56)	0.01324	-0.721248
C9JC84	FGG	Fibrinogen gamma chain	0.0338	-0.604038
E9PGN7	SERPING1	Plasma protease C1 inhibitor	0.01049	-0.588194
P03950	ANG	Angiogenin (EC 3.1.27.-) (Ribonuclease 5) (RNase 5)	0.00088	0.5947578
P02461	COL3A1	Collagen alpha-1(III) chain	0.04035	0.672549
A0A3B3IQ51	CFHR2	Complement factor H-related protein 2	0.02667	0.6738807
P62937	PPIA	Peptidyl-prolyl cis-trans isomerase A (PPIase A) (EC 5.2.1.8) (Cyclophilin A)	0.0214	0.7207679
P10586	PTPRF	Receptor-type tyrosine-protein phosphatase F (EC 3.1.3.48) (Leukocyte common antigen-related) (LAR)	0.0484	0.7680685
Q03591	CFHR1	Complement factor H-related protein 1 (FHR-1) (H factor-like protein 1) (H-factor-like 1) (H36)	0.0132	0.7800029
P59665	DEFA1	Neutrophil defensin 1 (Defensin, alpha 1)	0.01346	0.808495
P14174	MIF	Macrophage migration inhibitory factor (MIF) (EC 5.3.2.1)	0.04807	0.8522606
P13647	KRT5	Keratin, type II cytoskeletal 5 (58 kDa cytokeratin) (Cytokeratin-5) (CK-5) (Keratin-5) (K5)	0.00465	0.8602993
E9PIF4	NEU1	Exo-alpha-sialidase (EC 3.2.1.18)	0.04677	0.8623122
Q86YZ3	HRNR	Hornerin	0.01654	0.9364409
P13645	KRT10	Keratin, type I cytoskeletal 10 (Cytokeratin-10) (CK-10) (Keratin-10) (K10)	0.04081	1.0136109
P35908	KRT2	Keratin, type II cytoskeletal 2 epidermal (Cytokeratin-2e)	0.03029	1.0294628
Q9BXJ0	C1QTNF5	Complement C1q tumor necrosis factor-related protein 5	0.0158	1.0452895
Q07507	DPT	Dermatopontin (Tyrosine-rich acidic matrix protein) (TRAMP)	0.02807	1.3451692
P30838	ALDH3A1	Aldehyde dehydrogenase family 3 member A1	0.03002	1.6177392

Figure 2, Aqueous proteins profile by DIA-MS and DEPs abundant.

A, Volcano plot of the 875 quantified protein groups showing 10 down-regulated and 16 up-regulated protein groups for “Post group” versus “Pre group” comparison. 875 proteins were identification and quantification in AH by DIA-MS workflow and volcano plot showing 26 differentially expressed proteins (DEPs) in pre and post groups (|log2 (fold-change) | >0.58 and *p*-value <0.05). B, Heatmap showing hierarchical clustering of DEPs. C, The uniport ID, annotations, *P*-value, and log2 (fold-change) of 26 DEPs. FC, Fold changes of Post-group/Pre-group injection.

Table 1. Clinical characteristics of PDR patients for DIA-MS and ELISA analysis.

M, male; F, female; BP, blood pressure; IOP, intraocular pressure; VH, vitreous hemorrhage; TRD, tractional retinal detachment.

Patients	Age (years)	Gender	Diabetes course (years)	BP (mmHg）	surgical eye	vision	IOP (mmHg)	VH	TRD
1	30	M	6	154/94	OD	0.1c	19	Yes	No
2	36	F	12	128/79	OD	HM	12	Yes	Yes
3	56	F	9	127/87	OS	HM	14	Yes	Yes
4	52	M	10	121/82	OS	0.01	16	Yes	No
5	50	M	15	172/90	OD	CF/10cm	16	Yes	No
6	65	F	30	130/67	OD	CF/10cm	14	Yes	Yes
7	50	F	20	118/70	OD	HM	18	Yes	Yes
8	52	M	5	160/92	OD	CF/30cm	15	Yes	Yes
9	57	M	13	121/70	OS	CF/20cm	12	Yes	Yes
10	65	F	10	163/69	OD	0.05	16	Yes	Yes
11	47	M	1	115/65	OD	HM	11	Yes	Yes
12	43	M	10	121/75	OS	HM	15	Yes	Yes
13	53	M	20	166/88	OD	HM	18	Yes	Yes
14	61	F	12	159/95	OS	FC	14	Yes	Yes

3.2 Go annotation and pathway enrichment

To further understand the function of the differentially expressed proteins (DEPs) underlying the effect of intravitreal ranibizumab (IVR) in patients with proliferative diabetic retinopathy (PDR), we conducted gene ontology (GO) enrichment analysis and pathway analyses. Fisher's exact test (P adjust <0.05) was used to perform enrichment analysis of DEPs to determine the overall functional enrichment characteristics of all differentially expressed proteins and identify the most significant enriched pathway and GO terms.

Pathway analysis, including KEGG pathway, REACTOME pathway, and WikiPathways, revealed that the most notable pathway affected by IVR was "platelet degranulation," followed by "complement and coagulation cascades" and "neutrophil degranulation" (Figure 3A). GO annotation analysis identified 26 DEPs mainly associated with "extracellular matrix" terms, followed by "secretory granule lumen" and "platelet alpha granule lumen" (Figure 3B). To further explore the molecular function of the DEPs in response to IVR, GO molecular function annotation revealed that differentially expressed proteins were involved in extracellular matrix structural constituent, glycosaminoglycan binding, sulfur compound binding, cytokine activity, heparin binding, extracellular matrix binding, chemoattractant activity, scaffold protein binding, heparin binding, and structural constituent of skin epidermis (Figure 3C).

Among the DEPs, the differential expression of proteins related to the extracellular matrix caught our attention. Quantitative analysis via data-independent acquisition (DIA) methods showed that IVR treatment in PDR change the protein abundance levels of extracellular matrix components. The protein of angiogenin, collagen alpha-1 (COL3A1), DEFA1, Hornerin, and DPT, were up-regulated in response to IVR. Inversely, VEGFA, SPP1, LEFTY2, FCGBP, IMPG1, HTRA1, FGG, and plasma protease C1 inhibitor (SERPING1) were down-regulated (Figure 3D). Overall, our findings suggest that IVR affects various pathways and GO terms, with a significant impact on platelet degranulation and the extracellular matrix. The proteins related to the extracellular matrix may play a crucial role in the therapeutic effect of IVR in PDR patients.

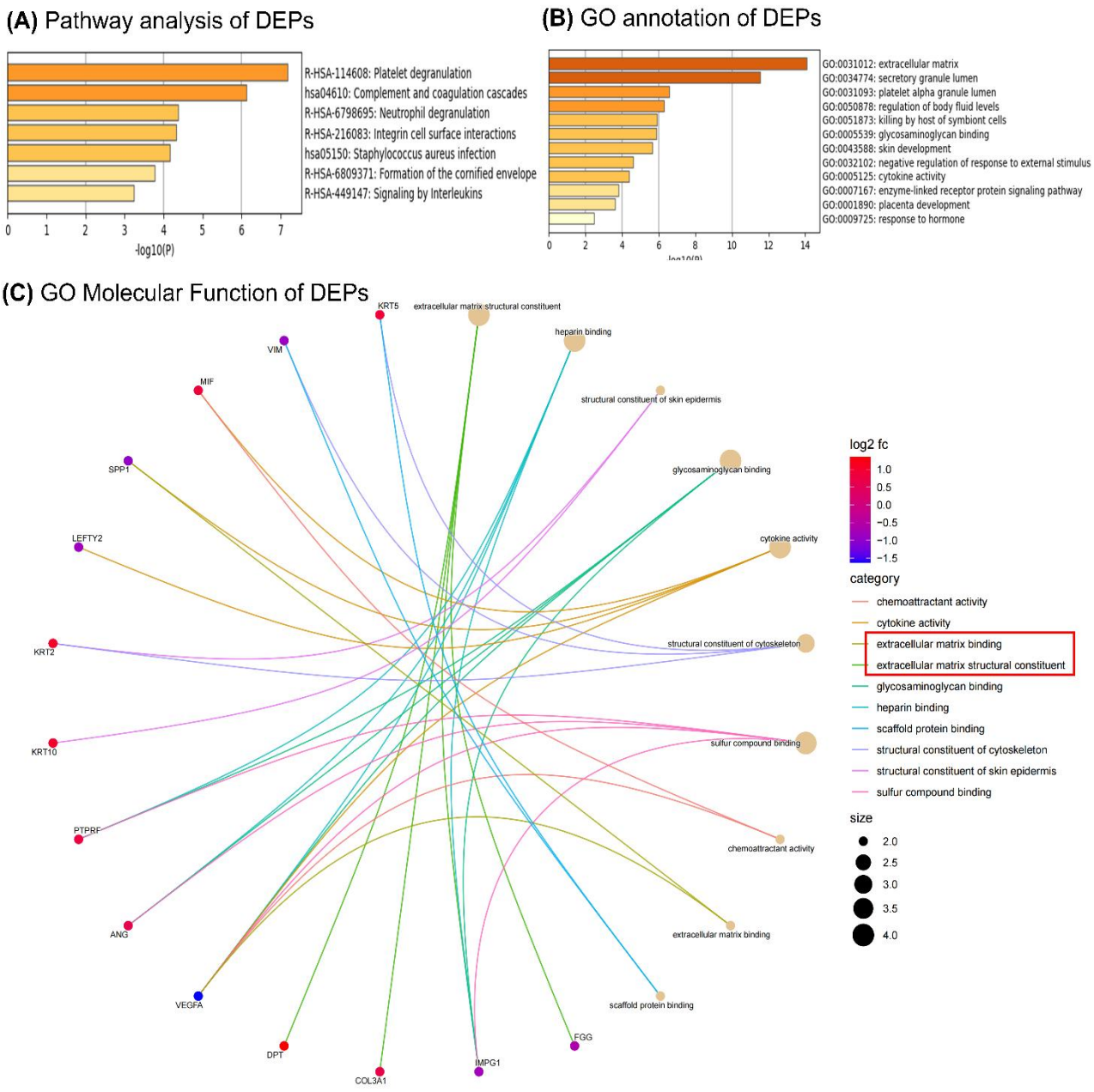
(A) Pathway analysis of DEPs
R-HSA-114608: Platelet degranulation
hsa04610: Complement and coagulation cascades
R-HSA-6798695: Neutrophil degranulation
R-HSA-216083: Integrin cell surface interactions
hsa05150: Staphylococcus aureus infection
R-HSA-6809371: Formation of the cornified envelope
R-HSA-449147: Signaling by Interleukins
-log10(P)
(B) GO annotation of DEPs
GO:0031012: extracellular matrix
GO:0034774: secretory granule lumen
GO:0031093: platelet alpha granule lumen
GO:0050878: regulation of body fluid levels
GO:0051873: killing by host of symbiont cells
GO:0005539: glycosaminoglycan binding
GO:0043588: skin development
GO:0032102: negative regulation of response to external stimulus
GO:0005125: cytokine activity
GO:0007167: enzyme-linked receptor protein signaling pathway
GO:0001890: placenta development
GO:0009725: response to hormone
(C) GO Molecular Function of DEPs
KRT5
extracellular matrix structural constituent
heparin binding
VIM
MIF
structural constituent of skin epidermis
SPP1
glycosaminoglycan binding
LEFTY2
cytokine activity
KRT12
structural constituent of cytoskeleton
KRT10
sulfur compound binding
PTPRF
chemoattractant activity
ANG
extracellular matrix binding
VEGFA
scaffold protein binding
FGG
DPT
IMPG1
COL3A1
log2 fc
1.0
0.5
0.0
−0.5
−1.0
−1.5
category
chemoattractant activity
cytokine activity
extracellular matrix binding
extracellular matrix structural constituent
glycosaminoglycan binding
heparin binding
scaffold protein binding
structural constituent of cytoskeleton
structural constituent of skin epidermis
sulfur compound binding
size
2.0
2.5
3.0
3.5
4.0
(D) Protein abundance levels of extracellular matrix components (Post-group/Pre-group)
log2FC
1.0
0.5
0.0
−0.5
−1.0
−1.5
Angiogenin
COL3A1
DEFA1
Homerin
DPT
VEGFA
SPP1
LEFTY2
FCGBP
IMPG1
HTRA1
FGG
SERPING1

Figure 3, GO and pathway analysis for DEPs of AH in response to IVR.

A, KEGG pathway, REACTOME pathway, and WikiPathways analysis of differentially expressed proteins. B, Gene Ontology (GO) enrichment analysis of differentially expressed proteins. C, GO molecular function annotation of differentially expressed proteins. D, Bar graph showing proteins abundance levels of extracellular matrix components by quantitative analysis via DIA methods. FC, Fold changes of Post-group/Pre-group injection.

3.3 Hub proteins analysis and validation.

To gain a deeper understanding of the relationship between differentially expressed proteins (DEPs), we conducted a protein-protein interaction (PPI) analysis using the STRING database and identified hub proteins using the Cytoscape tool. Through four different topological analysis methods (Degree, Edge Percolated Component (EPC), maximal clique centrality algorithm (MCC), and Closeness in Cytoscape plugin cytoHubba), we selected eight hub nodes, including VEGFA, DPT, SPP1, collagen alpha-1 (COL3A1), macrophage migration inhibitory factor (MIF), vimentin (VIM), peptidyl-prolyl cis-trans isomerase A (PPIA), and SERPING1 (Figure 4A, B).

Interestingly, among these eight hub proteins, VEGFA, SPP1, SERPING, COL3A1, and DPT were found to be involved in the extracellular matrix component. Furthermore, the expression differences in VEGFA and DPT proteins were particularly pronounced using the DIA method (Figure 3C). To validate these findings, enzyme-linked immunosorbent assay (ELISA) was performed on an additional set of aqueous samples collected from 4 patients with proliferative diabetic retinopathy (PDR) before and after intravitreal ranibizumab (IVR) treatment. In line with the previous findings, the ELISA results showed that the levels of VEGFA protein decreased ($P < 0.01$) and the levels of DPT increased ($P < 0.001$) in the aqueous humor of PDR patients after treatment with IVR (Figure 4C). These results indicate that IVR treatment can effectively reduce VEGFA protein expression and promote DPT protein content in the AH of PDR patients. Our analysis and validation of hub proteins

provide additional evidence for the alterations in VEGFA and DPT proteins in the AH of PDR patients following IVR treatment. It suggests that changes in these proteins may be associated with the therapeutic effects of IVR and could potentially serve as biomarkers for monitoring treatment response in PDR patients.

(A) The degree, EPC, MCC, and Closeness scores of hub proteins

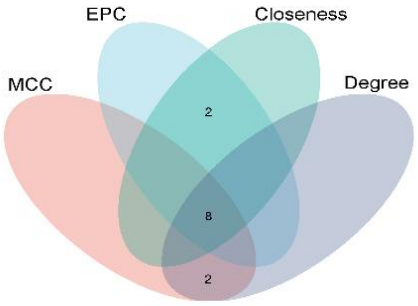

Gene	Degree	EPC	MCC	Closeness
SPP1	10	7	6	8
COL3A1	8	7	5	7
MIF	8	7	4	7
VIM	6	6	3	7
VEGFA	6	6	3	7
SERPING1	6	5	3	7
DPT	4	6	2	6
PPIA	4	6	2	6

(B) PPI network of DEPs

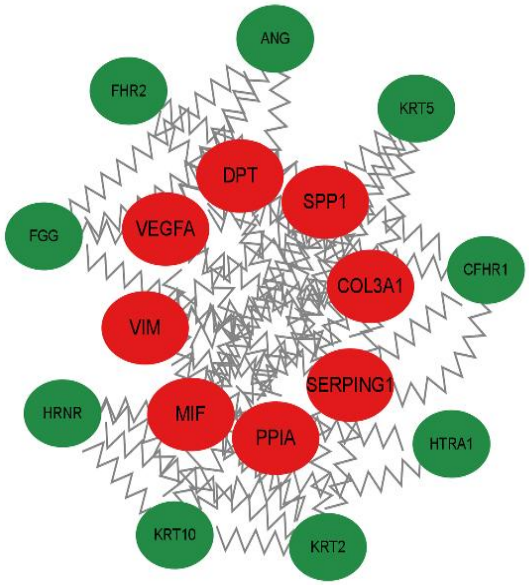

(C) The quantitative analysis of VEGFA and DPT protein in aqueous humor by ELISA

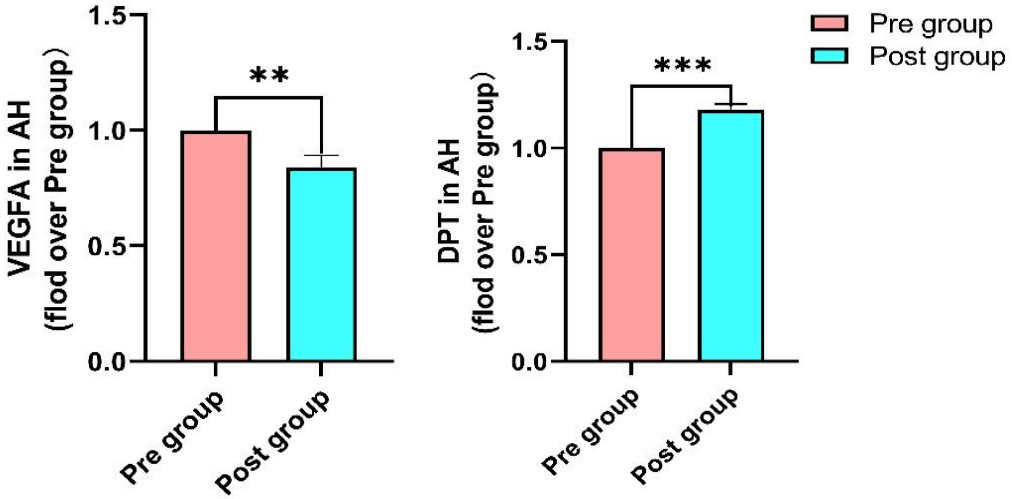

Figure 4, Hub proteins analysis and validation.

A, Hub proteins were selected using the Cytoscape tool with four algorithms: degree, EPC, MCC, and Closeness. The tatble shown the intersection of the outcomes from the four

algorithms. B, the protein-protein interaction network of DEPs in response to IVR. C, the levels of VEGFA and DPT protein in AH were measured by ELISA. The statistics are as follows: mean ±SEM, n=4. * $p < 0.05$, ** $p < 0.01$, *** $p < 0.001$. compared to the Pre group.

4. Discussion

Previous studies have pointed out a few potential molecules in PDR, however, the mechanisms of the anti-VEGF treatment in the retina remain not fully disentangled. Here, our study highlights the potential correlation between extracellular matrix dysfunction and VEGF signaling in PDR. In particular, our data first found the increase of DPT protein in the aqueous humor of PDR after IVR treatments, in which DPT may be a novel candidate target to improve retinal neovascularization and fibrosis combined with anti-VEGF therapy.

DR is a microvasculature complication in diabetes (Soni et al., 2021; Tonade & Kern, 2021), of which PDR is the sight-threatening stage led by retinal neovascularization and fibrovascular proliferation (Kang & Yang, 2020; Sahajpal et al., 2019). VEGF is a key angiogenic factor inducing neovascularization (Lawler, 2022), which is expressed by astrocytes, retinal pigment epithelial cells (RPE), ganglion cells, photoreceptor cells, and Müller cells (Li et al., 2019). Anti-VEGF therapy has become a common choice in the treatment of PDR (Mukwaya et al., 2021), however, several issues and underlying mechanisms remain unclear in the treatment of intravitreal anti-VEGF injection. Firstly, this treatment requires repeated, easily recurs angiogenesis, and places a large economic burden on patients (Liu et al., 2022; Mukwaya et al., 2021). Secondly, it can only maintain but not reverse or improve overall vision (Mukwaya et al., 2021). What's more, accumulating evidence has indicated that intravitreal injection of anti-VEGF agents may increase the risk of fibrosis to accelerate TRD (Chatziralli & Loewenstein, 2021; Liu et al., 2022; Tsui et al., 2023). Several molecules have been indicated as potential targets in PDR, such as PIGF, SPP1, APOC1, and ALDH3A1 in our and other studies(Chen, Qiu, et al., 2022; Hu et al., 2022; B. N. Zhang et al., 2021; Zhang et al., 2020; Zou, Han, et al., 2018; Zou, Zhao, et al., 2018). However, current research still does not fully explain the mechanisms and relationship between anti-VEGF therapy and fibrosis.

To fully explore the molecular mechanism of anti-VEGF therapy in PDR, DIA analysis was used to measure the proteomic change of AH between pre and post IVR treatment in PDR. In line with the vitreous humor study (Zou, Han, et al., 2018; Zou, Zhao, et al., 2018),

our data have found that the most notable pathway was “platelet degranulation” in AH of PDR compared with after anti-VEGF treatment. What’s more, GO annotation analysis showed the DEPs were mostly enrichment in “extracellular matrix” (ECM). The ECM, a non-cellular component, is a highly dynamic network of intercellular communication in all tissues and organs that serves not only as a physical scaffolding but also affords mechanical support and initiates pivotal biochemical and biomechanical cues to maintain tissue homeostasis (Corvera et al., 2022; Kai et al., 2019; Weiskirchen et al., 2019). The excessive deposition of ECM was the most key part of pathological architecture and a hallmarking in fibrosis (Pakshir & Hinz, 2018; Piersma et al., 2020). Water, proteoglycans, collagens, hyaluronan, and polysaccharides make up ECM (de Castro Brás & Frangogiannis, 2020; Mohan et al., 2020), while previous studies have indicated some components of ECM interaction with TGF-β signaling (Hachana & Larrivée, 2022; Mallone et al., 2021) to connect with ocular fibrosis and angiogenesis, such as integrins (Schulz et al., 2018; Van Hove et al., 2021), VEGFA (Lawler, 2022), fibronectin (Rocher et al., 2020), collagen (Lim et al., 2016), MMP(Yi et al., 2022) and so on. Therefore, the compositional variation of ECM may appear as a risk in fibrosis.

In our DEPs, the ECM components of DPT and COL3A1 were increased after IVR treatment and the protein of DPT has shown the greatest difference involved. Meanwhile, DPT and COL3A1 were also in the list of hub nodes. COL3A1 is a major fibrillar collagen of ECM, and the heterozygous mutations of the COL3A1 gene result in severe vascular diseases (Berezowska et al., 2018; D'Hondt et al., 2018; De Backer & De Backer, 2019). The extracellular matrix deposition can be relieved by the loss of COL3A1 expression (Lerner et al., 2020; H. Zhang et al., 2021).

What’s more, DPT protein, also known as tyrosine-rich acidic matrix protein (TRAMP), is predominantly found in the dermis of the skin and is an extensively distributed non-collagenous component of the ECM (Kim et al., 2019). It is involved in cell adhesion (Kramer et al., 2017), fibrosis (Wu et al., 2014), myogenesis (Kim et al., 2019), angiogenesis (Krishnaswamy et al., 2017), adipose tissue inflammation (Catalán et al., 2022), osteogenic proliferation and differentiation (Xi et al., 2018; Zhao et al., 2023), and tumor invasion and metastasis (Yamatoji et al., 2012). Combining DIA analysis and existing reports, we focused on the protein of DPT. Our data further demonstrated that anti-VEGF treatment can upregulate DPT expression and suppress the levels of VEGFA in the AH of PDR. Recently, several animal models have shown that new combination therapies by targeted VEGF with other factors (e.g., APOA1, pigment epithelium-derived factor (PEDF), leukocyte cell-derived chemotaxin 2 (LECT2)) were superior to anti-VEGF alone in reducing angiogenesis, neurodegeneration, and fibrosis (Lin et al., 2022; Xi, 2022; Zhang et al., 2022). Thus, this

makes DPT a novel target with great therapeutic promise which combines anti-VEGF therapy to further optimize the treatment outcomes of DR.

Except for DPT and COL3A1 protein, we also found the ECM proteins of VEGFA, SPP1, Fn1, SERPING1, and interphotoreceptor matrix proteoglycan 1 (IMPG1) were decreased after IVR treatment in PDR patients consistent with others (Youngblood et al., 2019), suggesting the protective function of anti-VEGF therapy. SPP1 is a multifunctional protein expressed in various cell types that acts both in intercellular interaction and the ECM to serve as an early driver of inflammation and long-term tissue damage in response to tumor growth and migration, angiogenesis, brain injury, immune reaction, and liver fibrosis (Song et al., 2021; Yim et al., 2022). It has been reported that SPP1 was increased in optic neuron degeneration (Ruzafa et al., 2018), and the down-regulation of SPP1 could reduce the generation of VEGF in the cornea (Fujita et al., 2010). As the main inhibitor of the classic complement system, lacking SERPING1 can lead to paroxysmal angioedema (Levi & Cohn, 2019; Shi & Wang, 2021), and the SERPING1 SNPs are a genetic risk factor for AMD and PCV (Liu et al., 2015).

In addition, the proteins of MIF, PPIA, and VIM were also in our hub proteins. MIF is a driver and pro-factor of inflammation, obesity, and insulin resistance tumors (Bozza et al., 2020; Penticuff et al., 2019). It has been reported that MIF and retinal angiogenesis have a positive correlation(Abu El-Asrar et al., 2019). With the inhibition of MIF, pathological damage responses can be blocked in retinal detachment (Kim et al., 2017). PPIAa is a rate-limiting enzyme in the protein folding reaction, whose activity is typically inhibited by cyclosporine A (CsA) (Cho et al., 2015). VIM is a mesenchymal marker interacting with SPP1 to induce cell division and migration in tumors (Ramos et al., 2020), and the existence of VIM promotes the degeneration of Müller glia cells (Hippert et al., 2021) and pigment epithelial cells (Llorián-Salvador et al., 2022) in the retina. Thus, we speculated that the increased protein of MIF and PPIA, and the decreased VIM in PDR with IVR treatment may be a reaction to the down of VEGFA. Meanwhile, similar to previously reported (Zou, Zhao, et al., 2018) that IVR treatment could increase the level of vitreous KRT1, we also found that the protein of keratin 2 (KRT2), keratin 5 (KRT5), and keratin 10 (KRT10) was upregulated in aqueous humor.

However, there were several limitations in our study. Firstly, this study was conducted on a limited number of patients and further verification of the mechanism (cells, animals, or populations) is needed; Secondly, the PDR can be sub-classified into early, high-risk, and severe PDR based on ETDRS Grading(Kroll et al., 2007), so studies on different degrees of PDR are warranted. Furthermore, other proteins such as APOA2, APOC1, TIMP2, and CP have shown a significant difference in vitreous humor in previous studies after IVR treatment in PDR (Zou, Han, et al., 2018; Zou, Zhao, et al., 2018) and were not in our DEPs list in AH.

The potential reasons are likely the differences in the organization itself of the aqueous and vitreous humor.

5. Conclusion

In summary, this study highlighted the changes of the ECM components in aqueous humor of PDR after IVR treatment, such as the up-regulated of DPT protein, which provide a clue between the anti-VEGF resistance and the exacerbation of fibrosis in PDR. Further exploration of the ECM pathway could enhance our comprehension of the molecular mechanisms driving angiogenesis and fibrosis, potentially leading to the development of new therapeutic strategies for PDR.

Acknowledgments

The authors thank the surgical team and the nurses of Peking Union Medical College Hospital for their invaluable assistance in collecting the samples. Additionally, the authors thank the websites https://www.iconfinder.com and https://www.pinclipart.com for providing the graphical materials used in this article. The availability of these resources has greatly enhanced the visual presentation of our findings.

Conflict of Interest

The authors declare that they have no conflict of interest.

Data Availability Statement

The data that support the findings of this study are available from the corresponding author upon reasonable request.

References

Abu El-Asrar, A. M., Ahmad, A., Siddiquei, M. M., De Zutter, A., Allegaert, E., Gikandi, P. W., De Hertogh, G., Van Damme, J., Opdenakker, G., & Struyf, S. (2019). The Proinflammatory and Proangiogenic Macrophage Migration Inhibitory Factor Is a Potential Regulator in

Proliferative Diabetic Retinopathy. *Front Immunol*, *10*, 2752. https://doi.org/10.3389/fimmu.2019.02752

Antonetti, D. A., Silva, P. S., & Stitt, A. W. (2021). Current understanding of the molecular and cellular pathology of diabetic retinopathy. *Nat Rev Endocrinol*, *17*(4), 195-206. https://doi.org/10.1038/s41574-020-00451-4

Berezowska, S., Christe, A., Bartholdi, D., Koch, M., & von Garnier, C. (2018). Pulmonary Fibrous Nodule with Ossifications May Indicate Vascular Ehlers-Danlos Syndrome with Missense Mutation in COL3A1. *Am J Respir Crit Care Med*, *197*(5), 661-662. https://doi.org/10.1164/rccm.201709-1963IM

Bons, J., Pan, D., Shah, S., Bai, R., Chen-Tanyolac, C., Wang, X., Elliott, D. R. F., Urisman, A., O'Broin, A., Basisty, N., Rose, J., Sangwan, V., Camilleri-Broët, S., Tankel, J., Gascard, P., Ferri, L., Tlsty, T. D., & Schilling, B. (2023). Data-independent acquisition and quantification of extracellular matrix from human lung in chronic inflammation-associated carcinomas. *Proteomics*, *23*(7-8), e2200021. https://doi.org/10.1002/pmic.202200021

Bozza, M. T., Lintomen, L., Kitoko, J. Z., Paiva, C. N., & Olsen, P. C. (2020). The Role of MIF on Eosinophil Biology and Eosinophilic Inflammation. *Clin Rev Allergy Immunol*, *58*(1), 15-24. https://doi.org/10.1007/s12016-019-08726-z

Catalán, V., Domench, P., Gómez-Ambrosi, J., Ramírez, B., Becerril, S., Mentxaka, A., Rodríguez, A., Valentí, V., Moncada, R., Baixauli, J., Silva, C., Escalada, J., & Frühbeck, G. (2022). Dermatopontin Influences the Development of Obesity-Associated Colon Cancer by Changes in the Expression of Extracellular Matrix Proteins. *Int J Mol Sci*, *23*(16). https://doi.org/10.3390/ijms23169222

Chatziralli, I., & Loewenstein, A. (2021). Intravitreal Anti-Vascular Endothelial Growth Factor Agents for the Treatment of Diabetic Retinopathy: A Review of the Literature. *Pharmaceutics*, *13*(8). https://doi.org/10.3390/pharmaceutics13081137

Chen, H., Qiu, B., Gao, G., Chen, Y., Min, H., & Wu, Z. (2022). Proteomic changes of aqueous humor in proliferative diabetic retinopathy patients treated with different intravitreal anti-VEGF agents. *Exp Eye Res*, *216*, 108942. https://doi.org/10.1016/j.exer.2022.108942

Chen, H., Wang, T., Wang, E., Li, N., & Min, H. (2022). Pursuing Diabetic Nephropathy through Aqueous Humor Proteomics Analysis. *Oxid Med Cell Longev*, *2022*, 5945828. https://doi.org/10.1155/2022/5945828

Chin, C. H., Chen, S. H., Wu, H. H., Ho, C. W., Ko, M. T., & Lin, C. Y. (2014). cytoHubba: identifying hub objects and sub-networks from complex interactome. *BMC Syst Biol*, *8 Suppl 4*(Suppl 4), S11. https://doi.org/10.1186/1752-0509-8-s4-s11

Cho, K. I., Orry, A., Park, S. E., & Ferreira, P. A. (2015). Targeting the cyclophilin domain of Ran-binding protein 2 (Ranbp2) with novel small molecules to control the proteostasis of STAT3, hnRNPA2B1 and M-opsin. *ACS Chem Neurosci*, *6*(8), 1476-1485. https://doi.org/10.1021/acschemneuro.5b00134

Corvera, S., Solivan-Rivera, J., & Yang Loureiro, Z. (2022). Angiogenesis in adipose tissue and obesity. *Angiogenesis*, *25*(4), 439-453. https://doi.org/10.1007/s10456-022-09848-3

D'Hondt, S., Guillemyn, B., Syx, D., Symoens, S., De Rycke, R., Vanhoutte, L., Toussaint, W.,

Lambrecht, B. N., De Paepe, A., Keene, D. R., Ishikawa, Y., Bächinger, H. P., Janssens, S., Bertrand, M. J. M., & Malfait, F. (2018). Type III collagen affects dermal and vascular collagen fibrillogenesis and tissue integrity in a mutant Col3a1 transgenic mouse model. *Matrix Biol*, *70*, 72-83. https://doi.org/10.1016/j.matbio.2018.03.008

De Backer, J., & De Backer, T. (2019). Vascular Ehlers-Danlos Syndrome Management: The Paris Way, A Step Forward on a Long Road. *J Am Coll Cardiol*, *73*(15), 1958-1960. https://doi.org/10.1016/j.jacc.2019.02.025

de Castro Brás, L. E., & Frangogiannis, N. G. (2020). Extracellular matrix-derived peptides in tissue remodeling and fibrosis. *Matrix Biol*, *91-92*, 176-187. https://doi.org/10.1016/j.matbio.2020.04.006

Dong, X., Lei, Y., Yu, Z., Wang, T., Liu, Y., Han, G., Zhang, X., Li, Y., Song, Y., Xu, H., Du, M., Yin, H., Wang, X., & Yan, H. (2021). Exosome-mediated delivery of an anti-angiogenic peptide inhibits pathological retinal angiogenesis. *Theranostics*, *11*(11), 5107-5126. https://doi.org/10.7150/thno.54755

Fujita, N., Fujita, S., Okada, Y., Fujita, K., Kitano, A., Yamanaka, O., Miyamoto, T., Kon, S., Uede, T., Rittling, S. R., Denhardt, D. T., & Saika, S. (2010). Impaired angiogenic response in the corneas of mice lacking osteopontin. *Invest Ophthalmol Vis Sci*, *51*(2), 790-794. https://doi.org/10.1167/iovs.09-3420

Hachana, S., & Larrivée, B. (2022). TGF-β Superfamily Signaling in the Eye: Implications for Ocular Pathologies. *Cells*, *11*(15). https://doi.org/10.3390/cells11152336

Hippert, C., Graca, A. B., Basche, M., Kalargyrou, A. A., Georgiadis, A., Ribeiro, J., Matsuyama, A., Aghaizu, N., Bainbridge, J. W., Smith, A. J., Ali, R. R., & Pearson, R. A. (2021). RNAi-mediated suppression of vimentin or glial fibrillary acidic protein prevents the establishment of Müller glial cell hypertrophy in progressive retinal degeneration. *Glia*, *69*(9), 2272-2290. https://doi.org/10.1002/glia.24034

Hu, Z., Cao, X., Chen, L., Su, Y., Ji, J., Yuan, S., Fransisca, S., Mugisha, A., Zou, W., Xie, P., & Liu, Q. (2022). Monitoring intraocular proangiogenic and profibrotic cytokines within 7 days after adjunctive anti-vascular endothelial growth factor therapy for proliferative diabetic retinopathy. *Acta Ophthalmol*, *100*(3), e726-e736. https://doi.org/10.1111/aos.14957

Kai, F., Drain, A. P., & Weaver, V. M. (2019). The Extracellular Matrix Modulates the Metastatic Journey. *Dev Cell*, *49*(3), 332-346. https://doi.org/10.1016/j.devcel.2019.03.026

Kang, Q., & Yang, C. (2020). Oxidative stress and diabetic retinopathy: Molecular mechanisms, pathogenetic role and therapeutic implications. *Redox Biol*, *37*, 101799. https://doi.org/10.1016/j.redox.2020.101799

Kim, B., Kusibati, R., Heisler-Taylor, T., Mantopoulos, D., Ding, J., Abdel-Rahman, M. H., Satoskar, A. R., Godbout, J. P., Bhattacharya, S. K., & Cebulla, C. M. (2017). MIF Inhibitor ISO-1 Protects Photoreceptors and Reduces Gliosis in Experimental Retinal Detachment. *Sci Rep*, *7*(1), 14336. https://doi.org/10.1038/s41598-017-14298-9

Kim, T., Ahmad, K., Shaikh, S., Jan, A. T., Seo, M. G., Lee, E. J., & Choi, I. (2019). Dermatopontin in Skeletal Muscle Extracellular Matrix Regulates Myogenesis. *Cells*, *8*(4). https://doi.org/10.3390/cells8040332

Kramer, A. C., Blake, A. L., Taisto, M. E., Lehrke, M. J., Webber, B. R., & Lund, T. C. (2017).

Dermatopontin in Bone Marrow Extracellular Matrix Regulates Adherence but Is Dispensable for Murine Hematopoietic Cell Maintenance. *Stem Cell Reports*, *9*(3), 770-778. https://doi.org/10.1016/j.stemcr.2017.07.021

Krishnaswamy, V. R., Balaguru, U. M., Chatterjee, S., & Korrapati, P. S. (2017). Dermatopontin augments angiogenesis and modulates the expression of transforming growth factor beta 1 and integrin alpha 3 beta 1 in endothelial cells. *Eur J Cell Biol*, *96*(3), 266-275. https://doi.org/10.1016/j.ejcb.2017.02.007

Kroll, P., Rodrigues, E. B., & Hoerle, S. (2007). Pathogenesis and classification of proliferative diabetic vitreoretinopathy. *Ophthalmologica*, *221*(2), 78-94. https://doi.org/10.1159/000098253

Lawler, J. (2022). Counter regulation of tumor angiogenesis by vascular endothelial growth factor and thrombospondin-1. *Semin Cancer Biol*, *86*(Pt 2), 126-135. https://doi.org/10.1016/j.semcancer.2022.09.006

Lerner, N., Schreiber-Avissar, S., & Beit-Yannai, E. (2020). Extracellular vesicle-mediated crosstalk between NPCE cells and TM cells result in modulation of Wnt signalling pathway and ECM remodelling. *J Cell Mol Med*, *24*(8), 4646-4658. https://doi.org/10.1111/jcmm.15129

Levi, M., & Cohn, D. M. (2019). The Role of Complement in Hereditary Angioedema. *Transfus Med Rev*, *33*(4), 243-247. https://doi.org/10.1016/j.tmrv.2019.08.002

Li, S., Guo, L., Zhou, P., Tang, J., Wang, Z., Zhang, L., Zhao, M., & Qu, J. (2022). Comparison of efficacy and safety of intravitreal ranibizumab and conbercept before vitrectomy in Chinese proliferative diabetic retinopathy patients: a prospective randomized controlled trial. *Eye Vis (Lond)*, *9*(1), 44. https://doi.org/10.1186/s40662-022-00316-z

Li, S., Tang, J., Han, X., Wang, Z., Zhang, L., Zhao, M., & Qu, J. (2022). Prospective Comparison of Surgery Outcome Between Preoperative and Intraoperative Intravitreal Injection of Ranibizumab for Vitrectomy in Proliferative Diabetic Retinopathy Patients. *Ophthalmol Ther*, *11*(5), 1833-1845. https://doi.org/10.1007/s40123-022-00550-7

Li, X., Liu, J., Hoh, J., & Liu, J. (2019). Müller cells in pathological retinal angiogenesis. *Transl Res*, *207*, 96-106. https://doi.org/10.1016/j.trsl.2018.12.006

Lim, R. R., Tan, A., Liu, Y. C., Barathi, V. A., Mohan, R. R., Mehta, J. S., & Chaurasia, S. S. (2016). ITF2357 transactivates Id3 and regulate TGFβ/BMP7 signaling pathways to attenuate corneal fibrosis. *Sci Rep*, *6*, 20841. https://doi.org/10.1038/srep20841

Lin, Y., Dong, M. Q., Liu, Z. M., Xu, M., Huang, Z. H., Liu, H. J., Gao, Y., & Zhou, W. J. (2022). A strategy of vascular-targeted therapy for liver fibrosis. *Hepatology*, *76*(3), 660-675. https://doi.org/10.1002/hep.32299

Liu, K., Lai, T. Y., Ma, L., Lai, F. H., Young, A. L., Brelen, M. E., Tam, P. O., Pang, C. P., & Chen, L. J. (2015). Ethnic differences in the association of SERPING1 with age-related macular degeneration and polypoidal choroidal vasculopathy. *Sci Rep*, *5*, 9424. https://doi.org/10.1038/srep09424

Liu, X., Liu, X., Wang, Y., Sun, H., Guo, Z., Tang, X., Li, J., Xiao, X., Zheng, S., Yu, M., He, C., Xu, J., & Sun, W. (2021). Proteome Characterization of Glaucoma Aqueous Humor. *Mol Cell Proteomics*, *20*, 100117. https://doi.org/10.1016/j.mcpro.2021.100117

Liu, Y., Yang, Q., Fu, H., Wang, J., Yuan, S., Li, X., Xie, P., Hu, Z., & Liu, Q. (2022). Müller glia-derived exosomal miR-9-3p promotes angiogenesis by restricting sphingosine-1-phosphate receptor S1P(1) in diabetic retinopathy. *Mol Ther Nucleic Acids*, *27*, 491-504. https://doi.org/10.1016/j.omtn.2021.12.019

Llorián-Salvador, M., Byrne, E. M., Szczepan, M., Little, K., Chen, M., & Xu, H. (2022). Complement activation contributes to subretinal fibrosis through the induction of epithelial-to-mesenchymal transition (EMT) in retinal pigment epithelial cells. *J Neuroinflammation*, *19*(1), 182. https://doi.org/10.1186/s12974-022-02546-3

Loukovaara, S., Nurkkala, H., Tamene, F., Gucciardo, E., Liu, X., Repo, P., Lehti, K., & Varjosalo, M. (2015). Quantitative Proteomics Analysis of Vitreous Humor from Diabetic Retinopathy Patients. *J Proteome Res*, *14*(12), 5131-5143. https://doi.org/10.1021/acs.jproteome.5b00900

Mallone, F., Costi, R., Marenco, M., Plateroti, R., Minni, A., Attanasio, G., Artico, M., & Lambiase, A. (2021). Understanding Drivers of Ocular Fibrosis: Current and Future Therapeutic Perspectives. *Int J Mol Sci*, *22*(21). https://doi.org/10.3390/ijms222111748

Matonti, F., Korobelnik, J. F., Dot, C., Gualino, V., Soler, V., Mrejen, S., Delyfer, M. N., Baillif, S., Streho, M., Gascon, P., Creuzot-Garcher, C., & Kodjikian, L. (2022). Comparative Effectiveness of Intravitreal Anti-Vascular Endothelial Growth Factor Therapies for Managing Neovascular Age-Related Macular Degeneration: A Meta-Analysis. *J Clin Med*, *11*(7). https://doi.org/10.3390/jcm11071834

Mohan, V., Das, A., & Sagi, I. (2020). Emerging roles of ECM remodeling processes in cancer. *Semin Cancer Biol*, *62*, 192-200. https://doi.org/10.1016/j.semcancer.2019.09.004

Mukwaya, A., Jensen, L., & Lagali, N. (2021). Relapse of pathological angiogenesis: functional role of the basement membrane and potential treatment strategies. *Exp Mol Med*, *53*(2), 189-201. https://doi.org/10.1038/s12276-021-00566-2

Pakshir, P., & Hinz, B. (2018). The big five in fibrosis: Macrophages, myofibroblasts, matrix, mechanics, and miscommunication. *Matrix Biol*, *68-69*, 81-93. https://doi.org/10.1016/j.matbio.2018.01.019

Penticuff, J. C., Woolbright, B. L., Sielecki, T. M., Weir, S. J., & Taylor, J. A., 3rd. (2019). MIF family proteins in genitourinary cancer: tumorigenic roles and therapeutic potential. *Nat Rev Urol*, *16*(5), 318-328. https://doi.org/10.1038/s41585-019-0171-9

Piersma, B., Hayward, M. K., & Weaver, V. M. (2020). Fibrosis and cancer: A strained relationship. *Biochim Biophys Acta Rev Cancer*, *1873*(2), 188356. https://doi.org/10.1016/j.bbcan.2020.188356

Ramos, I., Stamatakis, K., Oeste, C. L., & Pérez-Sala, D. (2020). Vimentin as a Multifaceted Player and Potential Therapeutic Target in Viral Infections. *Int J Mol Sci*, *21*(13). https://doi.org/10.3390/ijms21134675

Rocher, M., Robert, P. Y., & Desmoulière, A. (2020). The myofibroblast, biological activities and roles in eye repair and fibrosis. A focus on healing mechanisms in avascular cornea. *Eye (Lond)*, *34*(2), 232-240. https://doi.org/10.1038/s41433-019-0684-8

Ruzafa, N., Pereiro, X., Aspichueta, P., Araiz, J., & Vecino, E. (2018). The Retina of Osteopontin deficient Mice in Aging. *Mol Neurobiol*, *55*(1), 213-221. https://doi.org/10.1007/s12035-

017-0734-9

Sahajpal, N. S., Goel, R. K., Chaubey, A., Aurora, R., & Jain, S. K. (2019). Pathological Perturbations in Diabetic Retinopathy: Hyperglycemia, AGEs, Oxidative Stress and Inflammatory Pathways. *Curr Protein Pept Sci*, *20*(1), 92-110. https://doi.org/10.2174/1389203719666180928123449

Schulz, J. N., Plomann, M., Sengle, G., Gullberg, D., Krieg, T., & Eckes, B. (2018). New developments on skin fibrosis - Essential signals emanating from the extracellular matrix for the control of myofibroblasts. *Matrix Biol*, *68-69*, 522-532. https://doi.org/10.1016/j.matbio.2018.01.025

Shannon, P., Markiel, A., Ozier, O., Baliga, N. S., Wang, J. T., Ramage, D., Amin, N., Schwikowski, B., & Ideker, T. (2003). Cytoscape: a software environment for integrated models of biomolecular interaction networks. *Genome Res*, *13*(11), 2498-2504. https://doi.org/10.1101/gr.1239303

Sharma, I., Yadav, K. S., & Mugale, M. N. (2022). Redoxisome and diabetic retinopathy: Pathophysiology and therapeutic interventions. *Pharmacol Res*, *182*, 106292. https://doi.org/10.1016/j.phrs.2022.106292

She, X., Zou, C., & Zheng, Z. (2022). Differences in Vitreous Protein Profiles in Patients With Proliferative Diabetic Retinopathy Before and After Ranibizumab Treatment. *Front Med (Lausanne)*, *9*, 776855. https://doi.org/10.3389/fmed.2022.776855

Shi, Y., & Wang, C. (2021). Where we are with acquired angioedema due to C1 inhibitor deficiency: A systematic literature review. *Clin Immunol*, *230*, 108819. https://doi.org/10.1016/j.clim.2021.108819

Smith, J. M., & Steel, D. H. (2015). Anti-vascular endothelial growth factor for prevention of postoperative vitreous cavity haemorrhage after vitrectomy for proliferative diabetic retinopathy. *Cochrane Database Syst Rev*, *2015*(8), Cd008214. https://doi.org/10.1002/14651858.CD008214.pub3

Song, Z., Chen, W., Athavale, D., Ge, X., Desert, R., Das, S., Han, H., & Nieto, N. (2021). Osteopontin Takes Center Stage in Chronic Liver Disease. *Hepatology*, *73*(4), 1594-1608. https://doi.org/10.1002/hep.31582

Soni, D., Sagar, P., & Takkar, B. (2021). Diabetic retinal neurodegeneration as a form of diabetic retinopathy. *Int Ophthalmol*, *41*(9), 3223-3248. https://doi.org/10.1007/s10792-021-01864-4

Tan, Y., Fukutomi, A., Sun, M. T., Durkin, S., Gilhotra, J., & Chan, W. O. (2021). Anti-VEGF crunch syndrome in proliferative diabetic retinopathy: A review. *Surv Ophthalmol*, *66*(6), 926-932. https://doi.org/10.1016/j.survophthal.2021.03.001

Tonade, D., & Kern, T. S. (2021). Photoreceptor cells and RPE contribute to the development of diabetic retinopathy. *Prog Retin Eye Res*, *83*, 100919. https://doi.org/10.1016/j.preteyeres.2020.100919

Tsao, Y. T., Wu, W. C., Chen, K. J., Yeh, L. K., Hwang, Y. S., Hsueh, Y. J., Chen, H. C., & Cheng, C. M. (2021). Analysis of aqueous humor total antioxidant capacity and its correlation with corneal endothelial health. *Bioeng Transl Med*, *6*(2), e10199. https://doi.org/10.1002/btm2.10199

Tsui, J. C., Yu, Y., & VanderBeek, B. L. (2023). Association of Treatment Type and Loss to Follow-up With Tractional Retinal Detachment in Proliferative Diabetic Retinopathy. *JAMA Ophthalmol*, *141*(1), 40-46. https://doi.org/10.1001/jamaophthalmol.2022.4942

Van Hove, I., Hu, T. T., Beets, K., Van Bergen, T., Etienne, I., Stitt, A. W., Vermassen, E., & Feyen, J. H. M. (2021). Targeting RGD-binding integrins as an integrative therapy for diabetic retinopathy and neovascular age-related macular degeneration. *Prog Retin Eye Res*, *85*, 100966. https://doi.org/10.1016/j.preteyeres.2021.100966

Wang, D. Y., Zhao, X. Y., Zhang, W. F., Meng, L. H., & Chen, Y. X. (2020). Perioperative anti-vascular endothelial growth factor agents treatment in patients undergoing vitrectomy for complicated proliferative diabetic retinopathy: a network meta-analysis. *Sci Rep*, *10*(1), 18880. https://doi.org/10.1038/s41598-020-75896-8

Wang, T., Chen, H., Du, X., Li, N., Chen, Y., & Min, H. (2023). Differences in aqueous humor protein profiles in patients with proliferative diabetic retinopathy before and after conbercept treatment. *J Proteomics*, *276*, 104838. https://doi.org/10.1016/j.jprot.2023.104838

Weiskirchen, R., Weiskirchen, S., & Tacke, F. (2019). Organ and tissue fibrosis: Molecular signals, cellular mechanisms and translational implications. *Mol Aspects Med*, *65*, 2-15. https://doi.org/10.1016/j.mam.2018.06.003

Wu, W., Okamoto, O., Kato, A., Matsuo, N., Nomizu, M., Yoshioka, H., & Fujiwara, S. (2014). Dermatopontin regulates fibrin formation and its biological activity. *J Invest Dermatol*, *134*(1), 256-263. https://doi.org/10.1038/jid.2013.305

Xi, L. (2022). Combination of pigment epithelium derived factor with anti-vascular endothelial growth factor therapy protects the neuroretina from ischemic damage. *Biomed Pharmacother*, *151*, 113113. https://doi.org/10.1016/j.biopha.2022.113113

Xi, L. C., Ji, Y. X., Yin, D., Zhao, Z. X., Huang, S. C., Yu, S. L., Liu, B. Y., & Li, H. Y. (2018). Effects of Dermatopontin gene silencing on apoptosis and proliferation of osteosarcoma MG-63 cells. *Mol Med Rep*, *17*(1), 422-427. https://doi.org/10.3892/mmr.2017.7866

Yamatoji, M., Kasamatsu, A., Kouzu, Y., Koike, H., Sakamoto, Y., Ogawara, K., Shiiba, M., Tanzawa, H., & Uzawa, K. (2012). Dermatopontin: a potential predictor for metastasis of human oral cancer. *Int J Cancer*, *130*(12), 2903-2911. https://doi.org/10.1002/ijc.26328

Yi, C., Liu, J., Deng, W., Luo, C., Qi, J., Chen, M., & Xu, H. (2022). Macrophage elastase (MMP12) critically contributes to the development of subretinal fibrosis. *J Neuroinflammation*, *19*(1), 78. https://doi.org/10.1186/s12974-022-02433-x

Yim, A., Smith, C., & Brown, A. M. (2022). Osteopontin/secreted phosphoprotein-1 harnesses glial-, immune-, and neuronal cell ligand-receptor interactions to sense and regulate acute and chronic neuroinflammation. *Immunol Rev*, *311*(1), 224-233. https://doi.org/10.1111/imr.13081

Youngblood, H., Robinson, R., Sharma, A., & Sharma, S. (2019). Proteomic Biomarkers of Retinal Inflammation in Diabetic Retinopathy. *Int J Mol Sci*, *20*(19). https://doi.org/10.3390/ijms20194755

Zhang, B. N., Wu, X., Dai, Y., Qi, B., Fan, C., & Huang, Y. (2021). Proteomic analysis of aqueous humor from cataract patients with retinitis pigmentosa. *J Cell Physiol*, *236*(4), 2659-2668.

https://doi.org/10.1002/jcp.30031

Zhang, H., Ding, C., Li, Y., Xing, C., Wang, S., Yu, Z., Chen, L., Li, P., & Dai, M. (2021). Data mining-based study of collagen type III alpha 1 (COL3A1) prognostic value and immune exploration in pan-cancer. *Bioengineered*, *12*(1), 3634-3646. https://doi.org/10.1080/21655979.2021.1949838

Zhang, X., Wu, J., Wu, C., Bian, A. L., Geng, S., & Dai, R. P. (2020). Comparison of aqueous humor levels of PlGF and VEGF in proliferative diabetic retinopathy before and after intravitreal conbercept injection. *Diabetes Res Clin Pract*, *162*, 108083. https://doi.org/10.1016/j.diabres.2020.108083

Zhang, Z., Shen, M. M., & Fu, Y. (2022). Combination of AIBP, apoA-I, and Aflibercept Overcomes Anti-VEGF Resistance in Neovascular AMD by Inhibiting Arteriolar Choroidal Neovascularization. *Invest Ophthalmol Vis Sci*, *63*(12), 2. https://doi.org/10.1167/iovs.63.12.2

Zhao, X., Xie, Z., Rao, N., Zhang, S., & Zhang, Y. (2023). Effect of Dermatopontin on Osteogenic Differentiation of Periodontal Ligament Stem Cells. *Gene*, 147185. https://doi.org/10.1016/j.gene.2023.147185

Zou, C., Han, C., Zhao, M., Yu, J., Bai, L., Yao, Y., Gao, S., Cao, H., & Zheng, Z. (2018). Change of ranibizumab-induced human vitreous protein profile in patients with proliferative diabetic retinopathy based on proteomics analysis. *Clin Proteomics*, *15*, 12. https://doi.org/10.1186/s12014-018-9187-z

Zou, C., Zhao, M., Yu, J., Zhu, D., Wang, Y., She, X., Hu, Y., & Zheng, Z. (2018). Difference in the Vitreal Protein Profiles of Patients with Proliferative Diabetic Retinopathy with and without Intravitreal Conbercept Injection. *J Ophthalmol*, *2018*, 7397610. https://doi.org/10.1155/2018/7397610